Heliyon 6 (2020) e03683

Contents lists available at ScienceDirect

Heliyon

journal homepage: www.cell.com/heliyon

Research article

Free radical scavenging mechanism of 1,3,4-oxadiazole derivatives: thermodynamics of O–H and N–H bond cleavage

Ikechukwu Ogadimma Alisi [a,*], Adamu Uzairu [b], Stephen Eyije Abechi [b]

[a] Department of Applied Chemistry, Federal University Dutsinma, Katsina State, Nigeria
[b] Department of Chemistry, Ahmadu Bello University Zaria, Kaduna State, Nigeria

ARTICLE INFO

Keywords:
Organic chemistry
Physical chemistry
Gibbs free energy
Antioxidant
Reaction mechanism
Free radical scavenge
Virtual screening

ABSTRACT

The thermodynamics of free radical scavenge of 1,3,4-oxadiazole derivatives towards oxygen-centred free radicals were investigated by the density functional theory (DFT) method in the gas phase and aqueous solution. Three mechanisms of free radical scavenge namely, hydrogen atom transfer (HAT), single electron transfer followed by proton transfer (SET-PT) and sequential proton loss electron transfer (SPLET) were considered. The antioxidant descriptors that characterize these mechanisms such as, bond dissociation enthalpy (BDE), adiabatic ionization potential (AIP), proton dissociation enthalpy (PDE), proton affinity (PA) and electron transfer enthalpy (ETE) were evaluated. The sequence of electron donation as predicted by the HOMO results were in good agreement with the sequence of ETE for the considered molecules at their favoured sites of free radical scavenge. The reaction Gibbs free energy for inactivation of the selected peroxyl radicals, show that 1,3,4-oxadiazole antioxidants are more efficient radical scavengers by HAT and SPLET mechanisms than SET-PT mechanism in vacuum. In aqueous solution, the SET-PT mechanism was observed to be the dominant reaction pathway.

1. Introduction

The oxadiazoles are heterocyclic compounds that contain one oxygen and two nitrogen atoms in a five membered ring system. They exist in different isomeric forms such as 1,2,4-, 1,2,5-, 1,2,3- and 1,3,4-oxadiazoles. From recent studies, 1,3,4-oxadiazoles are an important class of heterocyclic compounds with a variety of biological activities such as anticancer [1, 2, 3, 4]; antibacterial [5, 6, 7]; anti-inflammatory [8, 9]; antifungal [10, 11, 12, 13, 14] and antioxidant [15, 16, 17, 18, 19] activities.

The technique of virtual screening is important as data bases to the design of novel compounds based on their biological activities [20]. Ligand-based methods rely on the assessment of physicochemical and structural similarities in a data set of molecules. The underlying principle is the assumption that similar ligands exert similar biological activities. These features could be obtained with the aid of quantitative structure activity relationship (QSAR) models, which explain the observed bioactivities in the considered compounds [21, 22].

Free radicals are generated in chemical systems when their atomic or molecular orbitals contain unpaired electrons [23]. When free radicals are generated in the body, they can be eradicated by an efficient antioxidant system. In recent time, there has been an increase in the prevalence of degenerative diseases caused by abnormal increase in the level of free radicals in the body [24]. This gives rise to oxidative stress which is the major cause of various health disorders such as: Diabetes, pulmonary failure, rheumatoid arthritis and renal failure [25]. Low levels of antioxidants in the human system necessitates the introduction of antioxidants from external sources into the body. This could be achieved through the intake of dietary supplements with highly efficient free radical scavenging potentials [26].

Three mechanisms are usually proposed to account for the free radical scavenging mechanism by antioxidants [27]. The first is hydrogen atom transfer (HAT). The second is single electron transfer followed by proton transfer (SET-PT). While, the third is sequential proton loss electron transfer (SPLET).

The aim of this work is to explore the free radical scavenging mechanisms of newly designed 1,3,4-oxadiazole derivatives by thermodynamic studies in the gas phase and aqueous solution. A set of 1,3,4-oxadiazole derivatives were designed by *in silico* virtual screening. This was achieved by employing the recently developed quantitative structure activity relationship, (QSAR) model for 1,3,4-oxadiazole antioxidants

* Corresponding author.
E-mail addresses: ikeogadialisi@gmail.com, ialisi@fudutsinma.edu.ng (I.O. Alisi).

https://doi.org/10.1016/j.heliyon.2020.e03683
Received 24 November 2019; Received in revised form 10 February 2020; Accepted 24 March 2020

[28]. The HAT, SET-PT and SPLET mechanisms of free radical scavenge were investigated by thermodynamic studies in this research.

2. Materials and methods

2.1. Ligand based virtual screening of 1,3,4-oxadiazole antioxidant derivatives

In the design of new set of 1,3,4-oxadiazole antioxidant derivatives bearing 2,3-dihydrobenzo [b] [1, 4]dioxine moiety, the method of ligand based virtual screening was employed. This was accomplished with the aid of the developed QSAR model for 1,3,4-oxadiazole antioxidants [29]. This model has an applicability domain leverage threshold h^*, value of 0.525.

With the aid of the developed QSAR model for 1,3,4-oxadiazole antioxidants, new set of 1,3,4-oxadiazole antioxidants were designed by insertion, deletion and substitution of various substituents on the template molecule [29, 30, 31, 32]. Subsequently, their antioxidant activities were predicted using this QSAR model. In the present research, compound M04 listed in Table 1 of Alisi *et al.* [28], whose structure is presented in Figure 1, was chosen as a template. The choice of this compound was based on its impressive antioxidant activity (pIC_{50} = 5.021) among the considered 1,3,4-oxadiazole antioxidant series.

The Chem Draw Program [33], was employed in drawing the chemical structures of the designed compounds. While, the minimization and subsequent optimization of the molecular structures were accomplished with the aid of Spartan 14 program [34], at the density functional theory (DFT), level using the Becke's three-parameter Lee-Yang-Parr hybrid functional (B3LYP), and 6-311G* basis set without symmetry constraints. Molecular descriptors for the optimized structures were obtained using the PADEL program package version 2.20 [35]. Subsequently, the leverage approach was employed in the assessment of the applicability domain of the designed 1,3,4-oxadiazoles.

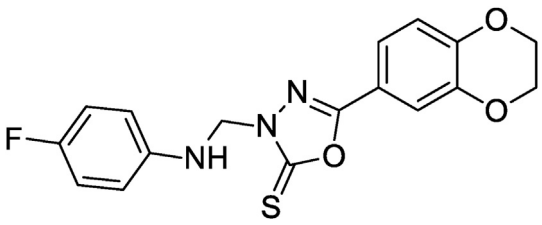

Figure 1. Parent 1,3,4-oxadiazole molecule (M04).

2.2. Computation of antioxidant descriptors

Evaluation of the preferred mechanism of free radical scavenge for the considered 1,3,4-oxadiazoles was accomplished by the computation of various antioxidant descriptors as presented below:

The homolytic bond dissociation enthalpy (BDE) was calculated under standard conditions of 1 atm. and 298.15 K using Eq. (1). BDE represents the standard reaction enthalpy change at a given temperature when a particular chemical bond is broken under standard conditions [32, 36]. Lower values of the BDE have been observed to favour lower stability of the O–H bond [37].

Table 1. Designed 1,3,4-oxadiazole antioxidant derivatives, their predicted antioxidant activities and leverage values.

Comp No	Designed antioxidants	pIC_{50}	Leverage
MOXM 01	3-(((3,5-difluoro-4-hydroxyphenyl)amino)methyl)-5-(5,8-dihydroxy-2,3-dihydrobenzo[b][1,4]dioxin-6-yl)-1,3,4-oxadiazole-2(3H)-thione	5.269	0.189
MOXM 02	3-(((4-amino-3,5-difluorophenyl)amino)methyl)-5-(5,8-diamino-2,3-dihydrobenzo[b][1,4]dioxin-6-yl)-1,3,4-oxadiazole-2(3H)-thione	5.418	0.245
MOXM 03	3-(((4-amino-3,5-difluorophenyl)amino)methyl)-5-(5,8-dihydroxy-2,3-dihydrobenzo[b][1,4]dioxin-6-yl)-1,3,4-oxadiazole-2(3H)-thione	5.275	0.151
MOXM 04	5-(5,8-diamino-2,3-dihydrobenzo[b][1,4]dioxin-6-yl)- 3-(((3,5-difluoro-4-hydroxyphenyl)amino)methyl)-1,3,4-oxadiazole-2(3H)-thione	5.450	0.219
MOXM 05	3-(((3,5-difluoro-4-hydroxyphenyl)amino)methyl)-5-(7-hydroxy-2,3-dihydrobenzo[b][1,4]dioxin-6-yl)-1,3,4-oxadiazole-2(3H)-thione	5.265	0.518
MOXM 06	3-(((2,6-difluoro-3,5-dihydroxy-4-methoxyphenyl)amino)methyl)-5-(2,3-dihydrobenzo[b][1,4]dioxin-6-yl)-1,3,4-oxadiazole-2(3H)-thione	4.884	0.234
MOXM 07	5-(8-amino-2,3-dihydrobenzo[b][1,4]dioxin-6-yl)-3-(((2,4,6-trifluoro-3,5-dihydroxyphenyl)amino)methyl)-1,3,4-oxadiazole-2(3H)-thione	5.101	0.115
MOXM 08	5-(8-hydroxy-2,3-dihydrobenzo[b][1,4]dioxin-6-yl)-3-(((2,4,6-trifluoro-3,5-dihydroxyphenyl)amino)methyl)-1,3,4-oxadiazole-2(3H)-thione	4.948	0.376
MOXM 09	5-(7-amino-2,3-dihydrobenzo[b][1,4]dioxin-6-yl)-3-(((2,4,6-trifluoro-3,5-dihydroxyphenyl)amino)methyl)-1,3,4-oxadiazole-2(3H)-thione	4.848	0.179
MOXM 10	5-(7-hydroxy-2,3-dihydrobenzo[b][1,4]dioxin-6-yl)-3-(((2,4,6-trifluoro-3,5-dihydroxyphenyl)amino)methyl)-1,3,4-oxadiazole-2(3H)-thione	4.797	0.224
MOXM 11	5-(5-amino-2,3-dihydrobenzo[b][1,4]dioxin-6-yl)-3-(((2,4,6-trifluoro-3,5-dihydroxyphenyl)amino)methyl)-1,3,4-oxadiazole-2(3H)-thione	4.931	0.103
MOXM 12	5-(5-hydroxy-2,3-dihydrobenzo[b][1,4]dioxin-6-yl)-3-(((2,4,6-trifluoro-3,5-dihydroxyphenyl)amino)methyl)-1,3,4-oxadiazole-2(3H)-thione	4.929	0.150
MOXM 13	3-(((3,5-diamino-2,4,6-trifluorophenyl)amino)methyl)-5-(8-hydroxy-2,3-dihydrobenzo[b][1,4]dioxin-6-yl)- 1,3,4-oxadiazole-2(3H)-thione	5.084	0.206
MOXM 14	5-(8-amino-2,3-dihydrobenzo[b][1,4]dioxin-6-yl)-3-(((3,5-diamino-2,4,6-trifluorophenyl)amino)methyl)-1,3,4-oxadiazole-2(3H)-thione	5.220	0.316
MOXM 15	3-(((3,5-diamino-2,4,6-trifluorophenyl)amino)methyl)-5-(7-hydroxy-2,3-dihydrobenzo[b][1,4]dioxin-6-yl)- 1,3,4-oxadiazole-2(3H)-thione	4.914	0.097
MOXM 16	5-(7-amino-2,3-dihydrobenzo[b][1,4]dioxin-6-yl)-3-(((3,5-diamino-2,4,6-trifluorophenyl)amino)methyl)-1,3,4-oxadiazole-2(3H)-thione	4.938	0.154
MOXM 17	3-(((3,5-diamino-2,4,6-trifluorophenyl)amino)methyl)-5-(5-hydroxy-2,3-dihydrobenzo[b][1,4]dioxin-6-yl)- 1,3,4-oxadiazole-2(3H)-thione	5.046	0.116
MOXM 18	5-(5-amino-2,3-dihydrobenzo[b][1,4]dioxin-6-yl)-3-(((3,5-diamino-2,4,6-trifluorophenyl)amino)methyl)-1,3,4-oxadiazole-2(3H)-thione	5.018	0.093
MOXM 19	5-(8-amino-2,3-dihydrobenzo[b][1,4]dioxin-6-yl)-3-(((2,3,5-trifluoro-4,6-dihydroxyphenyl)amino)methyl)-1,3,4-oxadiazole-2(3H)-thione	5.373	0.175
MOXM 20	5-(8-hydroxy-2,3-dihydrobenzo[b][1,4]dioxin-6-yl)-3-(((2,3,5-trifluoro-4,6-dihydroxyphenyl)amino)methyl)-1,3,4-oxadiazole-2(3H)-thione	5.335	0.182
MOXM 21	5-(7-amino-2,3-dihydrobenzo[b][1,4]dioxin-6-yl)-3-(((2,3,5-trifluoro-4,6-dihydroxyphenyl)amino)methyl)-1,3,4-oxadiazole-2(3H)-thione	5.111	0.139
MOXM 22	5-(7-hydroxy-2,3-dihydrobenzo[b][1,4]dioxin-6-yl)-3-(((2,3,5-trifluoro-4,6-dihydroxyphenyl)amino)methyl)-1,3,4-oxadiazole-2(3H)-thione	5.175	0.262
MOXM 23	5-(5-amino-2,3-dihydrobenzo[b][1,4]dioxin-6-yl)-3-(((2,3,5-trifluoro-4,6-dihydroxyphenyl)amino)methyl)-1,3,4-oxadiazole-2(3H)-thione	5.151	0.187
MOXM 24	5-(5-hydroxy-2,3-dihydrobenzo[b][1,4]dioxin-6-yl)-3-(((2,3,5-trifluoro-4,6-dihydroxyphenyl)amino)methyl)-1,3,4-oxadiazole-2(3H)-thione	5.247	0.239
MOXM 25	5-(8-amino-2,3-dihydrobenzo[b][1,4]dioxin-6-yl)-3-(((2,4-diamino-3,5,6-trifluorophenyl)amino)methyl)-1,3,4-oxadiazole-2(3H)-thione	5.310	0.146
MOXM 26	3-(((2,4-diamino-3,5,6-trifluorophenyl)amino)methyl)-5-(8-hydroxy-2,3-dihydrobenzo[b][1,4]dioxin-6-yl)- 1,3,4-oxadiazole-2(3H)-thione	5.250	0.127
MOXM 27	5-(7-amino-2,3-dihydrobenzo[b][1,4]dioxin-6-yl)-3-(((2,4-diamino-3,5,6-trifluorophenyl)amino)methyl)-1,3,4-oxadiazole-2(3H)-thione	5.021	0.433
MOXM 28	3-(((2,4-diamino-3,5,6-trifluorophenyl)amino)methyl)-5-(7-hydroxy-2,3-dihydrobenzo[b][1,4]dioxin-6-yl)- 1,3,4-oxadiazole-2(3H)-thione	5.077	0.264
MOXM 29	5-(5-amino-2,3-dihydrobenzo[b][1,4]dioxin-6-yl)-3-(((2,4-diamino-3,5,6-trifluorophenyl)amino)methyl)-1,3,4-oxadiazole-2(3H)-thione	5.169	0.077
MOXM 30	3-(((2,4-diamino-3,5,6-trifluorophenyl)amino)methyl)-5-(5-hydroxy-2,3-dihydrobenzo[b][1,4]dioxin-6-yl)- 1,3,4-oxadiazole-2(3H)-thione	5.157	0.083
MOXM 31	5-(5-amino-2,3-dihydrobenzo[b][1,4]dioxin-6-yl)-3-(((3,5-difluoro-4-hydroxyphenyl)amino)methyl)- 1,3,4-oxadiazole-2(3H)-thione	5.232	0.088

$$BDE = H_{radical} + H_H - H_{neutral} \quad (1)$$

The adiabatic ionization potential (AIP) was estimated as presented in Eq. (2). AIP describes the process of electron donation by the antioxidant, and represents the ability of the antioxidant to transfer electrons to the free radical. The lower the AIP value for a given molecule, the stronger the antioxidant properties.

$$AIP = H_{cation\ radical} + H_{electron} - H_{neutral} \quad (2)$$

The proton dissociation enthalpy (PDE) was also calculated using Eq. (3). PDE describes the ability of the compounds to donate proton. Molecules with lower PDE values have been found to be more susceptible to proton abstraction [38].

$$PDE = H_{radical} + H_{H^+} - H_{cation\ radical} \quad (3)$$

The proton affinity (PA) and electron transfer enthalpy (ETE) were also estimated using Eqs. (4) and (5) respectively.

$$PA = H_{anion} + H_{H^+} - H_{neutral} \quad (4)$$

$$ETE = H_{radical} + H_{electron} - H_{anion} \quad (5)$$

where.

$H_{radical}$ = Total enthalpy of phenoxyl radical.
H_H = Total enthalpy of the hydrogen atom.
$H_{neutral}$ = Total enthalpy of neutral compound.
H_{H^+} =Total enthalpy of the proton.
$H_{cation\ radical}$ = Total enthalpy of the cation radical.
$H_{electron}$ = Total enthalpy of the electron.
H_{anion} = Total enthalpy of the anion.

The total enthalpies of the species were calculated as the sum of total electronic energy, zero-point energy and the translational, rotational and vibrational contributions to the total enthalpy as presented in Eq. (6). In order to convert the energy to enthalpy, the RT (PV-work) term was added [39].

$$H = E_0 + ZPE + H_{trans} + H_{rot} + H_{vib} + RT \quad (6)$$

Where, H_{trans}, H_{rot}andH_{vib} are the translational, rotational, and vibrational contributions to the enthalpy respectively. E_0 is the total energy at 0 K while, ZPE is the zero-point vibrational energy.

Or the computation of the above antioxidant descriptors, the following values were employed: $H(H^{\bullet})_{vacuum}$ = -1312.479673 kJ/mol, $H(H^+)_{vacuum}$ = 6.1961805 kJ/mol, $H(e^-)_{vacuum}$ = 3.14534924 kJ/mol, $H(H^{\bullet})_{water}$ = − 3.9907603 kJ/mol, $H(H^+)_{water}$ = − 1090.00266 kJ/mol, $H(e^-)_{hydr}$ = − 105 kJ/mol [40, 41, 42, 43]. Geometry optimization of all molecular structures in the gas phase was performed at the DFT/B3LYP/6-311G* level of theory. Since water (ε = 78.39) is the physiological medium of human living cells, the solvation effect of water on the antioxidant activity was computed by using the self-consistent reaction field (SCRF) method with a polarized continuum model (PCM) [44, 45] at the DFT/B3LYP/6-31G* level.

2.3. Evaluation of the thermodynamically favoured mechanism

The reaction Gibbs free energy ($\Delta_r G$), results were employed in the evaluation of the thermodynamically favoured mechanism of free radical scavenge [46, 47]. In this research, the reaction Gibbs free energy of the reactants and products for the studied mechanisms of the reactions between the antioxidants and the two important peroxyl radicals; hydroperoxyl radical (HOO·) and methyl peroxyl radical (CH_3OO·) were investigated in the gas phase and aqueous solution.

The reaction between a free radical and an antioxidant is said to be thermodynamically favourable if the reaction Gibbs free energy is negative (Eq. (7)).

$$\Delta_r G = [G(products) - G(reactants)] < 0 \quad (7)$$

The reaction Gibbs free energy for the HAT mechanism is given by $\Delta_r G_{BDE}$ (Eq. (8)).

$$\Delta_r G_{BDE} = [G(H_{n-1}Antiox^{\bullet}) + G(RH)] - [G(H_nAntiox) + G(R^{\bullet})] \quad (8)$$

The reaction Gibbs free energy for the SET-PT mechanism is given by $\Delta_r G_{AIP}$ (Eq. (9)) and $\Delta_r G_{PDE}$ (Eq. (10)).

$$\Delta_r G_{AIP} = [G(H_{n-1}Antiox^{\bullet+}) + G(R^-)] - [G(H_nAntiox) + G(R^{\bullet})] \quad (9)$$

$$\Delta_r G_{PDE} = [G(H_{n-1}Antiox^{\bullet}) + G(RH)] - [G(H_{n-1}Antiox^{\bullet+}) + G(R^-)] \quad (10)$$

Also, the reaction Gibbs free energy for the SPLET mechanism is given by $\Delta_r G_{PA}$ (Eq. (11)) and $\Delta_r G_{ETE}$ (Eq. (12)).

$$\Delta_r G_{PA} = [G(H_{n-1}Antiox^-) + G(RH)] - [G(H_nAntiox) + G(R^-)] \quad (11)$$

$$\Delta_r G_{ETE} = [G(H_{n-1}Antiox^{\bullet}) + G(R^-)] - [G(H_{n-1}Antiox^-) + G(R^{\bullet})] \quad (12)$$

where.

$G(H_nAntiox)$: Gibbs free energy of neutral antioxidant.
$G(H_{n-1}Antiox^{\bullet})$: Gibbs free energy of phenoxyl radical.
$G(R^{\bullet})$: Gibbs free energy of free radical.
$G(HR)$: Gibbs free energy of product formed by hydrogen abstraction to free radical.
$G(H_{n-1}Antiox^{\bullet+})$: Gibbs free energy of cation radical.
$G(H^+)$: Gibbs free energy of proton.
$G(R^-)$: Gibbs free energy of free radical anion.
$G(H_{n-1}Antiox^-)$: Gibbs free energy of anion.

The values of $-3.72\ kJ/mol$ and $-26.28\ kJ/mol$ were employed as the Gibbs free energy of the electron (e^-) and proton (H^+) respectively in the gas phase. In aqueous solution, Gibbs free energy values of $-156.8\ kJ/mol$ and $-1104.5\ kJ/mol$ were used for the electron and proton respectively [48, 49].

3. Results and discussions

3.1. Analysis of ligand based virtual screening for 1,3,4-oxadiazole antioxidant derivatives

The pIC_{50} antioxidant activities and leverage values of the newly designed 1,3,4-oxadiazole antioxidants are presented in Table 1. The presented results show that majority of the designed compounds have better antioxidant activities compared to M04 ($pIC_{50} = 5.021$) which was used as the template compound. Also, from the computed leverage results, all the designed compounds were found within the applicability domain of the developed oxadiazole model which has a leverage threshold h^*, value of 0.525. This encouraging result indicates that no structural outliers were identified among the newly designed oxadiazole antioxidants. Subsequently, three of the designed compounds with best antioxidant activities (MOXM 04, MOXM 19 and MOXM 31) were subjected to thermodynamic studies. The structure and carbon atom numbering of these compounds are presented in Figure (2).

3.2. Analysis of the HAT mechanism

This is a mechanism in which H atom directly transfers from the antioxidant by homolytic O–H bond cleavage to the free radical to break oxidative chain reaction. BDE is the numerical parameter related to HAT mechanism and characterizes the stability of the corresponding hydroxyl group. A lower BDE value indicates that the stability of the corresponding O–H bond is lower and the corresponding O–H bond can be easily broken [37, 50]. This gives rise to higher antioxidant activity of the compound.

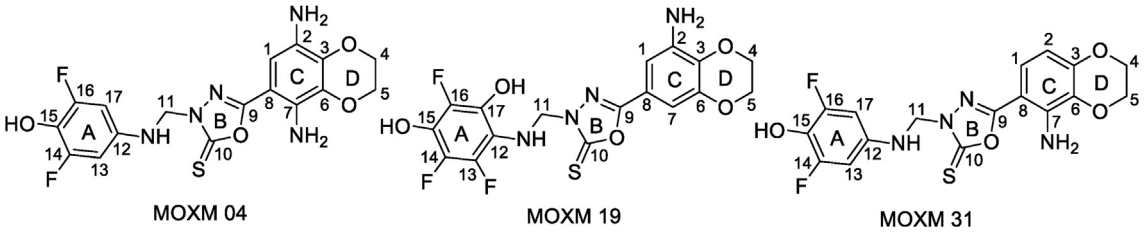

Figure 2. Molecular structure and carbon atom numbering of MOXM 04, MOXM 19 and MOXM 31.

Table 2 contains the results of BDE (KJ/mol) in the gas phase and aqueous solution for the different positions which are susceptible to hydrogen atom transfer for MOXM 04, MOXM 19 and MOXM 31. MOXM 04 and MOXM 19 molecules have four possible sites for hydrogen atom abstraction while, MOXM 31 molecule has three. For MOXM 04, the highest BDE was recorded at the 2-NH and 7-NH positions with values of 336.18 kJ/mol and 353.53 kJ/mol respectively in the gas phase. These results could be attributed to the susceptibility of these positions to form intramolecular hydrogen bonds with the adjacent alkoxy groups. MOXM 19 recorded the highest BDE at the 2NH position (361.41 kJ/mol). While MOXM 31 has the highest BDE at the 7NH position (381.68 kJ/mol). The high values of BDE recorded at these positions are also attributed to possible formation of intramolecular hydrogen bonds with their respective adjacent alkoxy groups. An examination of the BDE results for the three considered molecules MOXM 04, MOXM 19 and MOXM 31 in the gas phase shows that the lowest values of BDE are recorded at the 15-OH Position, except for MOXM 19 where a slightly lower value is recorded at the 17-OH position The variation of BDE for these molecules in vacuum is similar to that in aqueous solution. Although, the computed values in aqueous solution are higher. Based on this result, the 15-OH and 17-OH positions are the preferred sites of hydrogen atom transfer, for the considered 1,3,4-oxadiazole antioxidants. The BDE values at the preferred sites of HAT for MOXM 04 (294.72 kJ/mol and 1511.45 kJ/mol), MOXM 19 (286.53 kJ/mol and 1444.76 kJ/mol) and MOXM 31 (296.22 kJ/mol and 1508.82 kJ/mol) in vacuum and aqueous solution are lower than the BDE value of phenol (327.55 kJ/mol and 1632.72 kJ/mol) computed at the same level of theory, which is usually chosen as a reference compound. Consequently, these molecules are better free radical scavengers than phenol by HAT.

3.3. Analysis of the spin density distribution

In order to rationalize the observed differences in the values of BDE which resulted in differences in the reactivity of the various OH and NH_2 sites, the spin density distribution on the radicals of MOXM 04, MOXM 19 and MOXM 31 were calculated (Table 2). Lower radical spin density value indicates greater delocalization of the spin density in the radical, culminating in greater stability of the antioxidant radical, and subsequently, greater antioxidant activity of the compound [47, 51, 52]. Also, recall that the more delocalized the spin density in the radical, the easier the radical is formed, the lower the BDE. For MOXM 19, the order of radical spin density delocalization is, MOXM 19 2-NH· ˂ MOXM 19 11-NH· ˂ MOXM 19 15-O· ˂ MOXM 19 17-O·. This sequence is in agreement with the decreasing order of the BDE at these sites. For instance, MOXM 19 17-OH has the lowest spin density and BDE values of 2.34×10^{-4} and 286.53 kJ/mol respectively while, MOXM 19 2-NH has the highest spin density and BDE values of 6.96×10^{-4} and 361.41 kJ/mol respectively. Subsequently, based on the results of spin density distribution as presented in Table 2, the most feasible site for the formation of MOXM 19 radical is at the 17-OH site, while, the least is the 2-NH site. Similarly, the preferred site of radical formation for MOXM 04 and MOXM 31 molecules is the 15-OH site.

3.4. Analysis of the SET-PT mechanism

The adiabatic ionization potential (AIP) and the proton dissociation enthalpy (PDE) parameters for the studied molecules in vacuum and aqueous solution are presented in Table 2. The first step of the SET-PT mechanism is characterized by the result of the AIP. For MOXM 04 molecule, the lowest values of AIP in vacuum were recorded at the 2-NH and 7-NH sites with very close values of 368.83 kJ/mol and 369.06 kJ/mol respectively. For the molecules of MOXM 19 and MOXM3, the lowest AIP results were obtained at the11-NH site with values of 378.49 kJ/mol and 393.95 kJ/mol respectively. These results imply that the electron donating abilities of these molecules are more favoured at the above stated sites. Recall that the lower the AIP value for a given molecule, the higher the electron donating ability. Also the AIP values for the studied molecules at all the possible sites are significantly lower than that of phenol (572.78 kJ/mol) at the same level of theory except for MOXM 19 15-OH (575.24 kJ/mol). Thus the electron donating abilities of these

Table 2. Antioxidant properties of designed 1,3,4-oxadiazole antioxidant derivatives calculated at the B3LYP/6-311G* level in vacuum and in water.

Comp No	BDE (kJ/mol)		AIP (kJ/mol)		PDE (kJ/mol)		PA (kJ/mol)		ETE (kJ/mol)		Radical Spin Density
	Gas	Water	Gas	Water	Gas	Water	Gas	Water	Gas	Water	
MOXM 04 2-NH	336.18	1686.83	368.83	-1001.87	1289.17	1497.69	1513.60	509.71	144.40	-13.90	6.12×10^{-4}
MOXM 04 7-NH	353.53	1730.94	369.06	-1024.19	1306.29	1564.11	1484.22	497.11	191.13	42.82	5.23×10^{-4}
MOXM 04 11-NH	334.21	1690.51	388.25	-996.10	1267.78	1495.59	1457.18	464.56	198.85	34.94	4.85×10^{-4}
MOXM 04 15-OH	294.72	1511.45	545.52	-951.46	1071.02	1271.90	1423.36	239.81	193.18	80.62	2.95×10^{-4}
MOXM 19 2-NH	361.41	1703.37	432.55	-976.14	1250.68	1488.50	1493.86	472.17	189.37	40.19	6.96×10^{-4}
MOXM 19 11-NH	335.99	1681.84	378.49	-1028.13	1279.33	1518.96	1406.61	400.49	251.20	90.34	5.04×10^{-4}
MOXM 19 15-OH	288.76	1460.78	575.24	-946.74	1035.34	1216.50	1394.30	147.66	216.28	122.11	2.66×10^{-4}
MOXM 19 17-OH	286.53	1444.76	392.93	-1050.97	1215.42	1304.72	1388.84	138.47	219.51	115.28	2.34×10^{-4}
MOXM 31 7-NH	381.68	1731.20	401.85	-1002.40	1301.64	1542.59	1470.04	462.19	233.45	78.00	6.58×10^{-4}
MOXM 31 11-NH	333.66	1673.44	393.95	-995.83	1261.53	1478.26	1455.42	444.08	200.06	38.35	4.87×10^{-4}
MOXM 31 15-OH	296.22	1508.82	548.88	-951.72	1069.16	1269.53	1422.36	261.60	195.67	56.21	2.95×10^{-4}
Phenol	327.55	1632.72	572.78	-1132.24	1076.59	1497.69	1462.89	141.47	186.48	300.24	

molecules are stronger than that of phenol. The AIP values in water are lower than those in vacuum. In aqueous solution, the values of AIP unlike BDE seem to be more influenced by the solvent polarity since the latter may affect charge separation in a molecule. The higher IP values in vacuum in comparison to that in aqueous solution suggest that SET is not favored in vacuum.

PDE characterize the second step of the SET-PT mechanism. The lowest results of PDE obtained for MOXM 04 (1071.02 kJ/mol and 1271.90 kJ/mol) MOXM 19 (1035.34 kJ/mol and 1216.50 kJ/mol) and MOXM 31 (1069.16 kJ/mol and 1269.53 kJ/mol) occurred at the 15-OH position in vacuum and water respectively. These results are lower than that of phenol in vacuum and water (1076.59 kJ/mol and 1497.69 kJ/mol) which is usually chosen as a reference molecule. Therefore, the most favoured site for proton dissociation for all the three molecules is the 15-OH position. The observed trend of PDE is analogous to that of BDE for the title molecules (Table 2). This could be attributed to the fact that proton dissociation results in the formation of the antioxidant radical as with bond dissociation. For reaction mechanisms that involve multiple steps such as the SET-PT mechanism, the first step in this case AIP, is the most important from thermodynamics view point. The above results suggest that SET-PT mechanism is more favoured in aqueous solution compared to the gas phase.

3.5. Analysis of the SPLET mechanism

The observed results of proton affinity (PA) and electron transfer enthalpy (ETE) for MOXM 04, MOXM 19 and MOXM 31 1,3,4-oxadiazole antioxidants molecules in vacuum and water are presented in Table 2. The first step of SPLET mechanism is characterized by PA, while the second step is characterized by ETE. A lower PA value favours the deprotonation of the oxadiazole antioxidant to give the phenoxyl anion. An examination of the PA results in the two media for the 1,3,4-oxadiazole molecules indicates that the preferred site for deprotonation is the 15-OH position with values of 1423.36 kJ/mol and 239.81 kJ/mol; 1394.30 kJ/mol and 147.66 kJ/mol; and 1422.37 kJ/mol and 261.60 kJ/mol for MOXM 04, MOXM 19 and MOXM 31 in vacuum and water respectively. The only exception occurs at t 17OH position where a slightly lower value is observed.

The lower the ETE value, the more active is the resulting phenoxide anion for a given molecule [32]. The ETE results in vacuum as presented in Table 2 reveal that the 15-OH position in ring A is the preferred site for the second step of the SPLET mechanism for MOXM 31 1,3,4-oxadiazole antioxidant as judged by the lowest ETE value of 195.67 kJ/mol obtained at this position. For MOXM 04 and MOXM 19 molecules, the preferred site is the 2-NH position with ETE values of 144.40 kJ/mol and 189.37 kJ/mol respectively. A similar trend is observed in aqueous solution. In vacuum, the ETE value at each molecular site is observed to be lower than that of AIP (Table 2). This shows that single electron transfer from the anionic form is more favourable than that from the neutral form. This result is in agreement with previous research [42, 51, 52].

As stated earlier, for multiple step mechanisms such as SPLET, the first step in this case, the deprotonation of the 1,3,4-oxadiazole antioxidant molecule is the most important. Observe that the preferred site for HAT is the same as that of SPLET for each molecule.

3.6. Thermodynamically preferred mechanism

The reaction Gibbs free energy for scavenging HOO· and CH_3OO· via HAT, SET-PT and SPLET mechanisms by the selected 1,3,4-oxadiazole antioxidants in vacuum and water are reported in Tables 3 and 4 respectively. As stated earlier, more negative reaction Gibbs free energy ($\Delta_r G$) results represent the thermodynamically more favoured reactions. Therefore, results from the computation of $\Delta_r G$could be helpful in the assignment of the free radical scavenging potency of molecules. For each of the molecules, MOXM 04, MOXM 19 and MOXM 31 in vacuum, reaction feasibility for the deactivation of HOO· via HAT and SPLET mechanisms were observed at the 15-OH position (Table 3). For MOXM 19, a more feasible site was predicted at the 17OH position (Table 3). The feasibility of these positions is attributed to the exergonicity of their $\Delta_r G$ reactions. A similar trend is obsserved in aqueous solution.

From Table 3, the first step of the SPLET mechanism ($\Delta_r G_{PA}$) at these positions is exergonic, while the second step is endergonic. In this case, since the exergonicity of $\Delta_r G_{PA}$ overwhelms the endergonicity of $\Delta_r G_{ETE}$ and PA is the first step of the SPLET mechanism, the resulting SPLET mechanism is therefore exergonic at the 15-OH for each of MOXM 04, MOXM 19 and MOXM 31 including the 17-OH position for MOXM 19. In addition, a thermodynamically unfeasible reaction could be driven by a thermodynamically feasible reaction. Similar results of the radical scavenge of HOO· at the above mentioned positions for each molecule are observed for the radical scavenge of CH_3OO· radical as presented in Table 4. For the SET-PT reaction pathway, the first step ($\Delta_r G_{AIP}$) is endergonic while, the second step ($\Delta_r G_{PDE}$) is exergonic in vacuum. Consequently, this mechanism is thermodynamically unfeasible in this phase.

With respect to the SET-PT mechanism, a different trend is observed in aqueous solution where $\Delta_r \boldsymbol{G_{AIP}}$ is exergonic, while $\Delta_r \boldsymbol{G_{PDE}}$ is endergonic in the presence of both HOO· than CH_3OO· radicals at all positions for the three molecules. Consequently, the SET-PT mechanism I thermodynamically feasible in aqueous solution. Among all the considered molecules, MOXM 04 at the 2NH site recoded the highest negative $\Delta_r \boldsymbol{G_{AIP}}$ value for scavenging HOO· radical. This mechanism is presented in Scheme 1 (c).

Table 3. Gibbs free energy changes ($\Delta_r G$ in kJ/mol) of scavenging HOO· radical by 1,3,4-oxadiazole antioxidant derivatives at the B3LYP/6-311G* level in vacuum and in water.

Comp No	HAT		SET-PT				SPLET			
	$\Delta_r \boldsymbol{G_{BDE}}$		$\Delta_r \boldsymbol{G_{AIP}}$		$\Delta_r \boldsymbol{G_{PDE}}$		$\Delta_r \boldsymbol{G_{PA}}$		$\Delta_r \boldsymbol{G_{ETE}}$	
	Gas	Water	Gas	Water	Gas	Water	Gas	Water	Gas	Water
MOXM 04 2-NH	15.65	40.57	502.08	-74287.09	-486.42	74327.66	-121.19	86.12	136.84	-45.56
MOXM 04 7-NH	32.88	55.79	499.35	-74270.02	-466.47	74325.81	-151.31	90.85	184.18	-35.06
MOXM 04 11-NH	13.16	44.24	520.35	-74233.00	-507.19	74277.25	-179.48	45.95	192.64	-1.71
MOXM 04 15-OH	-26.28	-152.41	674.13	-74181.28	-700.40	74028.87	-210.54	-242.07	184.26	89.66
MOXM 19 2-NH	40.78	72.34	562.99	-74281.58	-522.21	74353.91	-141.46	56.98	182.24	15.35
MOXM 19 11-NH	14.97	24.81	510.30	-74246.66	-495.32	74271.47	-228.36	11.04	243.33	13.78
MOXM 19 15-OH	-31.19	-176.04	704.98	-74194.15	-736.16	74018.11	-240.52	-281.97	209.33	105.93
MOXM 19 17-OH	-33.71	-167.90	523.74	-74224.34	-557.44	74056.44	-246.35	-268.06	212.64	100.16
MOXM 31 7-NH	61.99	82.05	534.08	-74268.98	-472.09	74351.03	-164.35	61.71	226.35	20.34
MOXM 31 11-NH	13.63	26.65	526.26	-74243.24	-512.63	74269.90	-179.69	27.58	193.32	-0.92
MOXM 31 15-OH	-23.94	-158.97	679.01	-74191.26	-702.95	74032.29	-210.85	-195.86	186.91	36.88

Table 4. Gibbs free energy changes ($\Delta_r G$ in kJ/mol) of scavenging $CH_3OO\cdot$ radical by 1,3,4-oxadiazole antioxidant derivatives at the B3LYP/6-311G* level in vacuum and in water.

Comp No	HAT		SET-PT				SPLET			
	$\Delta_r G_{BDE}$		$\Delta_r G_{AIP}$		$\Delta_r G_{PDE}$		$\Delta_r G_{PA}$		$\Delta_r G_{ETE}$	
	Gas	Water	Gas	Water	Gas	Water	Gas	Water	Gas	Water
MOXM 04 2-NH	18.89	43.19	464.06	-573668.47	-445.16	74328.83	-79.93	87.30	98.82	-44.10
MOXM 04 7-NH	36.11	58.42	461.32	-573651.40	-425.21	74326.99	-110.05	92.02	146.16	-33.60
MOXM 04 11-NH	16.40	46.87	482.33	-573614.38	-465.93	74278.42	-138.22	47.13	154.61	-0.26
MOXM 04 15-OH	-23.04	-149.78	636.10	-573562.66	-659.14	74030.05	-169.28	-240.89	146.24	91.11
MOXM 19 2-NH	44.02	74.96	524.97	-573662.96	-480.95	74355.09	-100.20	58.16	144.22	16.81
MOXM 19 11-NH	18.21	27.44	472.27	-573628.04	-454.06	74272.64	-187.10	12.21	205.31	15.23
MOXM 19 15-OH	-27.95	-173.41	666.95	-573575.53	-694.90	74019.28	-199.26	-280.80	171.31	107.39
MOXM 19 17-OH	-30.47	-165.27	485.72	-573605.72	-516.18	74057.62	-205.09	-266.88	174.62	101.61
MOXM 31 7-NH	65.23	84.68	496.06	-573650.36	-430.83	74352.20	-123.09	62.88	188.32	21.80
MOXM 31 11-NH	16.87	29.28	488.24	-573624.62	-471.37	74271.07	-138.43	28.75	155.30	0.53
MOXM 31 15-OH	-20.70	-156.34	640.99	-573572.64	-661.69	74033.46	-169.59	-194.68	148.89	38.34

. A comparison of the results in Table 3 to those of Table 4 indicate that the investigated 1,3,4-oxadiazole antioxidants have higher potential to scavenge HOO· than $CH_3OO\cdot$ via HAT and SPLET mechanisms in vacuum and SET-PT mechanism in water. The results presented in Tables 3 and 4 indicate that MOXM 19 exhibited best results for $\Delta_r G$ at the 15-OH site in comparison to MOXM 04 and MOXM 31. Consequently, the HAT and SPLET mechanisms for scavenging HOO· radical by MOXM 19 15-OH are presented in Scheme 1 (a) and (b) respectively.

3.7. Analysis of frontier molecular orbital distribution

The frontier orbital distribution and energy for MOXM 04, MOXM 19 and MOXM 31 were calculated at the B3LYP/6-311G* level in the gas phase and presented in Figure 3. The distribution of LUMO in the three molecules presents similar results. The LUMO is localized on ring C in each molecule. Therefore, this is the region that is more susceptible to electron gain. The HOMO distribution for the three molecules are different. For MOXM 04, the HOMO is localized on ring C and the two amino groups attached to this ring. For MOXM 19, it is distributed on rings B and C. While that of MOXM 31 is on ring A. From the results presented in Figure 3, MOXM 04, MOXM 19 and MOXM 31 have HOMO values of -5.19 eV, -5.76 eV and -5.67 eV respectively. Based on this result, MOXM 04 has the highest electron donating ability while, MOXM 19 has the weakest electron donating ability mong the three considered molecules. This trend is in good agreement with the sequence of ETE of these molecules at the 15-OH sites for each of the molecules MOXM 04, MOXM 31 and MOXM 19. This corresponds to the favoured sites of free radical scavenge as predicted by the Gibbs free energy results (Tables 3 and 4). Recall that the excitation of an electron from a molecule is favoured by higher HOMO energy value [51, 52, 53].

The HOMO-LUMO energy gap (E Gap) results are presented in Figure 3. MOXM 04 has the lowest E Gap value of 3.76 eV. Since reactivity of a molecule is favoured by lower values of E Gap, MOXM 04 is predicted to be the most reactive and subsequently, have the best

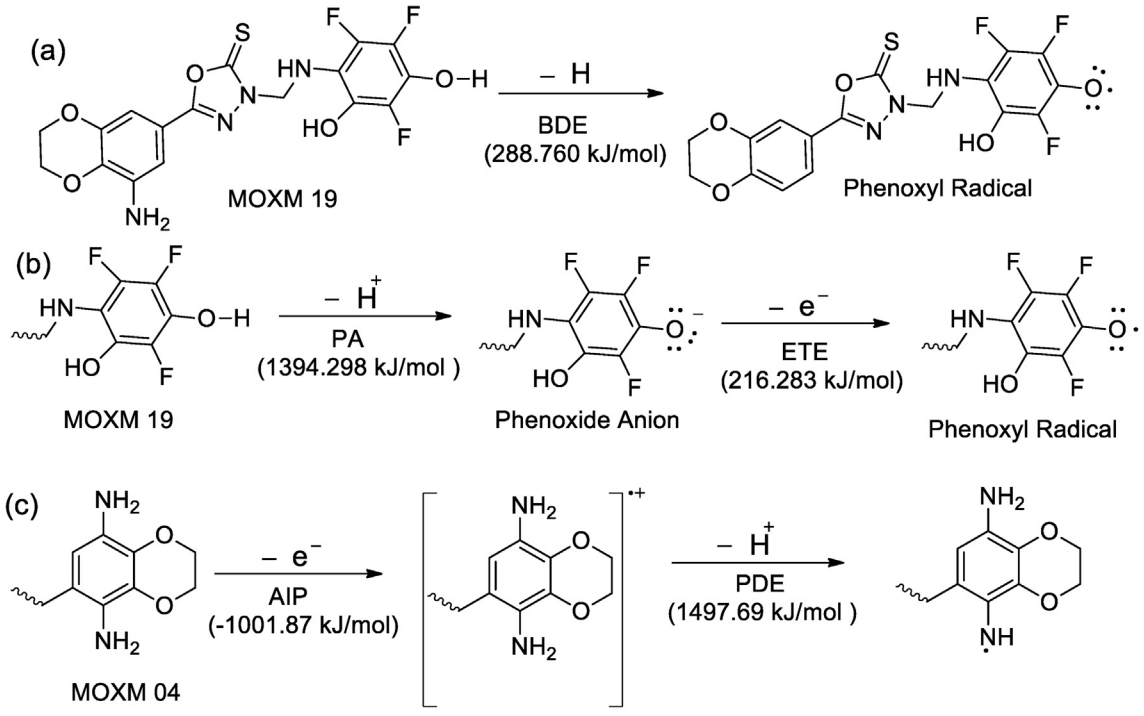

Scheme 1. (a) HAT mechanism of MOXM 19 in vacuum and water. (b) SPLET mechanism of MOXM 19 in vacuum and water. (c) SET-PT mechanism of MOXM 04 in water.

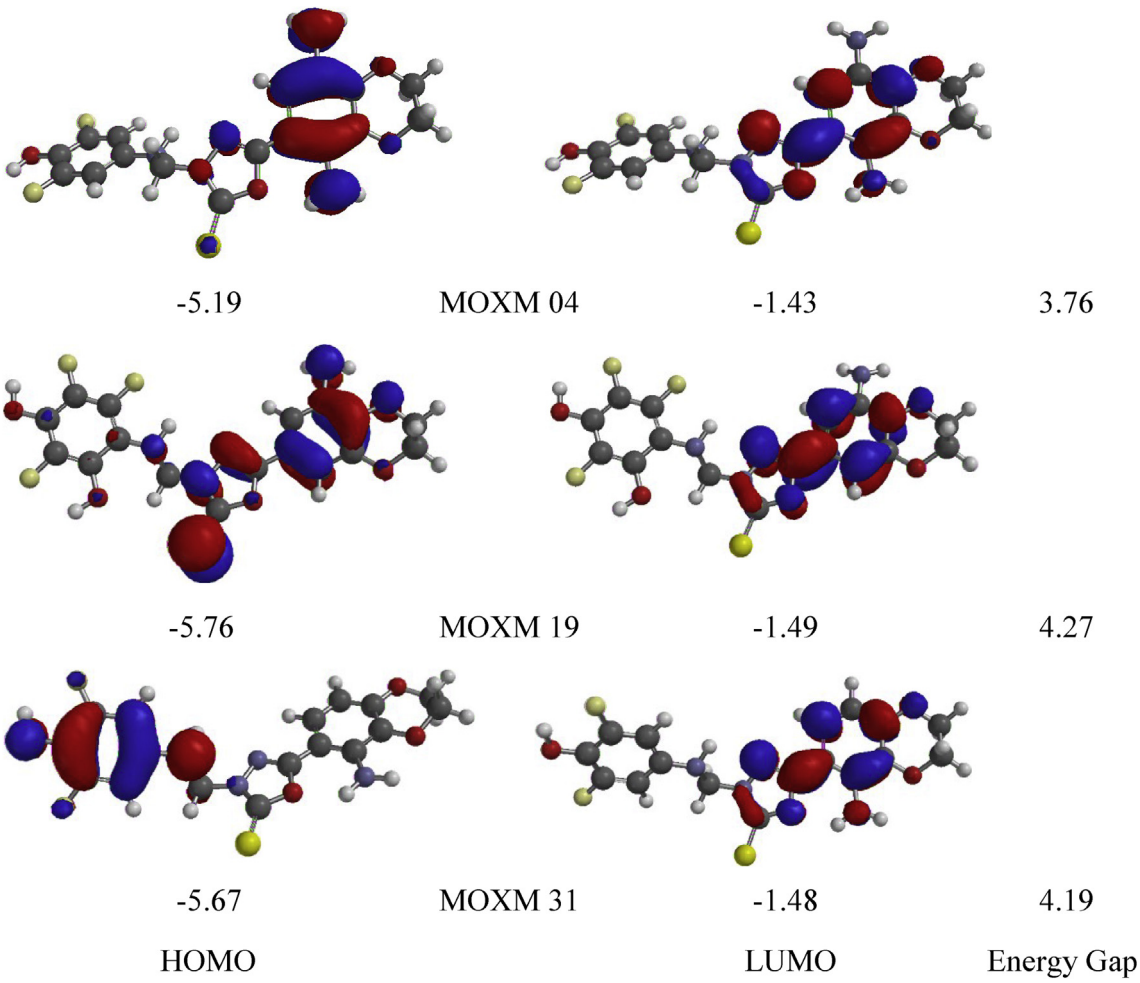

Figure 3. The orbital distribution and energy (in eV) of HOMO and LUMO for MOXM 04, MOXM 19 and MOXM 31computed at the B3LYP/6-311G* level in the gas phase.

antioxidant activity among the three molecules. These results are in good agreement with the predicted antioxidant activity as presented in Table 1.

4. Conclusion

This research entails the application of *in silico* virtual screening in the design of new set of1,3,4-oxadiazole antioxidants. A total of 31 antioxidants were designed and their free radical scavenging activities and leverage values determined using the developed antioxidant model for 1,3,4-oxadiazoles. The free radical scavenging mechanisms of the three molecules with best antioxidant activities were investigated by thermodynamics studies.

The HAT, SET-PT and SPLET mechanisms of free radical scavenge were investigated by computing their various reaction enthalpies such as BDE, AIP, PDE, PA and ETE. Calculations in aqueous solution indicated an increase in the BDE values for the considered molecules compared the computed values in vacuum. In order to explain the observed differences in the BDE values, the spin density distribution of the radicals were calculated. Also, the frontier orbital energies of the three molecules were computed. Among the three considered molecules, MOXM 19 at the 15-OH and 17-OH sites, possessed the greatest ability to transfer hydrogen atom to the free radical based on their lowest values for BDE (288.76 kJ/mol and 286.53 kJ/mol respectively). Also, electron transfer from the anionic form of the antioxidant is more favourable than that from the neutral form based on the computed results of ETE and AIP.

The reaction Gibbs free energy results computed for each of the molecules MOXM 04, MOXM 19 and MOXM 31 facilitated the prediction of their thermodynamically plausible mechanisms of free radical scavenge. It was observed the HAT and SPLET mechanisms were thermodynamically feasible reaction pathways for MOXM 04, MOXM 19 and MOXM 31 at their 15-OH sites in vacuum. For MOXM 19 an additional position with thermodynamic feasibility was observed at 17-OH site. In aqueous solution, the SET-PT mechanism was the dominant reaction pathway. The exergonicity of the observed results for the three mechanisms reveal that these oxadiazole compounds are more efficient in scavenging HOO· than CH_3OO· This research is a gateway towards an efficient exploitation of antioxidant potentials of 1,3,4-oxadiazoles in the fields of food chemistry and pharmacy.

Declarations

Author contribution statement

Ikechukwu Ogadimma Alisi, Adamu Uzairu and Stephen Eyije Abechi: Conceived and designed the experiments; The three authors analyzed and interpreted the data; Ikechukwu Alisi wrote the paper.

Funding statement

This research did not receive any specific grant from funding agencies in the public, commercial, or not-for-profit sectors.

Competing interest statement

The authors declare no conflict of interest.

Additional information

No additional information is available for this paper.

Acknowledgements

The authors are grateful to the physical and theoretical chemistry teams in Ahmadu Bello University Zaria and Federal University Dutsinma for their assistance and cooperation.

References

[1] F.A.F. Ragab, S.M. Abou-Seri, S.A. Abdel-Aziz, A.M. Alfayomy, M. Aboelmagd, Design, synthesis and anticancer activity of new monastrol analogues bearing 1,3,4-oxadiazole moiety, Eur. J. Med. Chem. 138 (2017) 140–151.
[2] T. Globe, K. Szymankiewicz, P. Swiatek, Anti-cancer activity of derivatives of 1,3,4-oxadiazole, Molecules 23 (12) (2018) 3361.
[3] A. Ahmad, H. Varshney, A. Rauf, A. Sherwani, M. Owais, Synthesis and anticancer activity of long chain substituted 1,3,4-oxadiazol-2-thione, 1,2,4-triazol-3-thione and 1,2,4-triazolo[3,4-b]-1,3,4-thiadiazine derivatives, Arabian J. Chem. 10 (2017) S3347–S3357.
[4] W. Caneschi, K.B. Enes, C. Carvalho de Mendonça, F. de Souza Fernandes, F.B. Miguel, J. da Silva Martins, M.R. Costa Couri, Synthesis and anticancer evaluation of new lipophilic 1,2,4 and 1,3,4-oxadiazoles, Eur. J. Med. Chem. 165 (2019) 18–30.
[5] J.P. Raval, T.N. Akhaja, D.M. Jaspara, K.N. Myangar, N.H. Patel, Synthesis and in vitro antibacterial activity of new oxoethylthio-1,3,4-oxadiazole derivatives, J. Saudi Chem. Soc. 18 (2) (2014) 101–106.
[6] X. Song, P. Li, M. Li, A. Yang, L. Yu, L. Luo, D. Hu, B. Song, Synthesis and investigation of the antibacterial activity and action mechanism of 1,3,4-oxadiazole thioether derivatives, Pestic. Biochem. Physiol. 147 (2018) 11–19.
[7] Y. Guo, T. Xu, C. Bao, Z. Liu, J. Fan, R. Yang, S. Qin, Design and synthesis of new norfloxacin-1,3,4-oxadiazole hybrids as antibacterial agents against methicillin-resistant Staphylococcus aureus (MRSA), Eur. J. Pharmaceut. Sci. 136 (2019) 104966.
[8] H.S. Abd-Ellah, M. Abdel-Aziz, M.E. Shoman, E.A.M. Beshr, T. Kaoud, S.F.F. Ahmed, New 1,3,4-oxadiazole/oxime hybrids: design, synthesis, anti-inflammatory, COX inhibitory activities and ulcerogenic liability, Bioorg. Chem. 74 (2017) 15–29.
[9] S.A. Popov, M.D. Semenova, D.S. Baev, I.V. Sorokina, N.A. Zhukova, T.S. Frolova, M. Turks, Lupane-type conjugates with aminoacids, 1,3,4- oxadiazole and 1,2,5-oxadiazole-2-oxide derivatives: synthesis, anti-inflammatory activity and in silico evaluation of target affinity, Steroids 150 (2019) 108443.
[10] M.Y. Wani, A. Ahmad, R.A. Shiekh, K.J. Al-Ghamdi, A.J.F.N. Sobral, Imidazole clubbed 1,3,4-oxadiazole derivatives as potential antifungal agents, Bioorg. Med. Chem. 23 (15) (2015) 4172–4180.
[11] X. Wang, X. Fu, J. Yan, A. Wang, M. Wang, M. Chen, C. Yang, Y. Song, Design and synthesis of novel 2-(6-thioxo-1,3,5-thiadiazinan-3-yl)-N′-phenylacethydrazide derivatives as potential fungicides, Mol. Divers. 23 (3) (2018) 573–583.
[12] X. Wang, H. Hu, X. Zhao, M. Chen, T. Zhang, C. Geng, Y. Mei, A. Lu, C. Yang, Novel quinazolin-4(3H)-one derivatives containing a 1,3,4-oxadiazole thioether moiety as potential bactericides and fungicides: design, synthesis, characterization and 3D-QSAR analysis, J. Saudi Chem. Soc. 23 (8) (2019) 1144–1156.
[13] X. Wang, X. Fu, M. Chen, A. Wang, J. Yan, Y. Mei, M. Wang, C. Yang, Novel 1,3,5-thiadiazine-2-thione derivatives containing a hydrazide moiety: design, synthesis and bioactive evaluation against phytopathogenic fungi in vitro and in vivo, Chin. Chem. Lett. 30 (7) (2019) 1419–1422.
[14] J. Jiao, A. Wang, M. Chen, M. Wang, C. Yang, Novel 5-choro-pyrazole derivatives containing a phenylhydrazone moiety as potent antifungal agents: synthesis, crystal structure, biological evaluation and 3D-QSAR study, New J. Chem. 43 (2019) 6350–6360.
[15] A.C. Sauer, J.G. Leal, S.T. Stefanello, M.T.B. Leite, M.B. Souza, F.A.A. Soares, O.E.D. Rodrigues, L. Dornelles, Synthesis and antioxidant properties of organosulfur and organoselenium compounds derived from 5-substituted-1,3,4-oxadiazole/thiadiazole-2-thiols, Tetrahedron Lett. 58 (1) (2017) 87–91.
[16] M. Malhotra, R.K. Rawal, D. Malhotra, R. Dhingra, A. Deep, P.C. Sharma, Synthesis, characterization and pharmacological evaluation of (Z)-2-(5-(biphenyl-4-yl)-3-(1-(imino)ethyl)-2,3-dihydro-1,3,4-oxadiazol-2-yl)phenol derivatives as potent antimicrobial and antioxidant agents, Arabian J. Chem. 10 (1) (2017) S1022–S1031.
[17] Y.U. Cebeci, H. Bayrak, Y. Şirin, Synthesis of novel schiff bases and azol-β-lactam derivatives starting from morpholine and thiomorpholine and investigation of their antitubercular, antiurease activity, acethylcolinesterase inhibition effect and antioxidant capacity, Bioorg. Chem. (2019) 102928.
[18] K. Jakovljević, I.Z. Matić, T. Stanojković, A. Krivokuća, V. Marković, M.D. Joksović, N. Mihailovic, M. Niciforovic, L. Joksović, Synthesis, antioxidant and antiproliferative activities of 1,3,4-thiadiazoles derived from phenolic acids, Bioorg. Med. Chem. Lett 27 (16) (2017) 3709–3715.
[19] K. Jakovljević, M.D. Joksović, B. Botta, L.S. Jovanović, E. Avdović, Z. Marković, V. Mihailovic, M. Andric, S. Trifunovic, V. Marković, Novel 1,3,4-thiadiazole conjugates derived from protocatechuic acid: synthesis, antioxidant activity, and computational and electrochemical studies, C. R. Chim. 22 (8) (2019) 585–598.
[20] V. Vivek, J. Anurekha, J. Avijeet, G. Arun, Virtual screening: a fast tool for drug design, Sci. Pharm. 76 (3) (2008) 333–360.
[21] A.I. Ogadimma, U. Adamu, Quantitative structure activity relationship analysis of selected chalcone derivatives as mycobacterium tuberculosis inhibitors, OALib 3 (2016), e2432.
[22] I.O. Alisi, A. Uzairu, S.E. Abechi, S.O. Idris, Evaluation of the antioxidant properties of curcumin derivatives bygenetic function algorithm, J. Adv. Res. 12 (2018) 47–54.
[23] I.O. Alisi, A. Uzairu, S.E. Abechi, S.O. Idris, Free radical scavenging activity evaluation of hydrazones by quantitative structure activity relationship, J. Mex. Chem. Soc. 62 (1) (2018) 1–13.
[24] G. Firpo, M.L. Ramírez, M.S. Faillace, M. de Brito, R.M. dos, A.P.S.C.L. Silva, J.P. Costa, W.J. Peláez, Evaluation of the antioxidant activity of cis/trans-N-phenyl-1,4,4a,5,8,8a-hexahydro-3,1-benzoxazin-2-imines, Antioxidants 8 (6) (2019) 197.
[25] A. Galano, A.J. Raul, Computational strategies for predicting free radical scavengers' protection againstoxidative stress: where are we and what might follow? Int. J. Quant. Chem. 119 (2019), e25665.
[26] R. Paramaguru, P.M. Mazumder, D. Sasmal, D. Kumar, K. Mukhopadhyay, Evaluation of antioxidant and DNA nicking potential along with HPTLC fingerprint analysis of different parts of Pterospermumacerifolium (L.) Willd, Free Radic. Antioxidants 3 (2) (2013) 100–106.
[27] Y. Li, M. Toscano, G. Mazzone, N. Russo, Antioxidant properties and free radical scavenging mechanisms of cyclocurcumin, New J. Chem. 42 (15) (2018) 12698–12705.
[28] I. Alisi, A. Uzairu, S. Abechi, S. Idris, Development of predictive antioxidant models for 1,3,4-oxadiazoles by quantitative structure activity relationship, JOTCSA 6 (2) (2019) 103–114.
[29] G. Melagraki, A. Afantitis, H. Sarimveis, P.A. Koutentis, G. Kollias, O. Igglessi-Markopoulou, Predictive QSAR workflow for the in silico identification and screening of novel HDAC inhibitors, Mol. Divers. 13 (3) (2009) 301–311.
[30] T. Asadollahi, S. Dadfarnia, A.M.H. Shabani, J.B. Ghasemi, M. Sarkhosh, QSAR models for CXCR2 receptor antagonists based on the genetic algorithm for data preprocessing prior to application of the PLS linear regression method and design of the new compounds using *in Silico* virtual screening, Molecules 16 (2011) 1928–1955.
[31] I. Mitra, A. Saha, K. Roy, Chemometric QSAR modeling and in Silico design of antioxidant NO donor phenols, Sci. Pharm. 79 (2011) 31–58.
[32] I.O. Alisi, A. Uzairu, S.E. Abechi, In silico design of hydrazone antioxidants and analysis of their free radical-scavenging mechanism by thermodynamic studies, Beni-Suef Univ. J. Basic Appl. Sci. 8 (11) (2019) 1–11.
[33] Z. Li, H. Wan, Y. Shi, P. Ouyang, Personal experience with four kinds of chemical structure drawing software: review on ChemDraw, ChemWindow, ISIS/Draw, and ChemSketch, J. Chem. Inf. Comput. Sci. 44 (5) (2004) 1886–1890.
[34] Y. Shao, L.F. Molnar, Y. Jung, J. Kussmann, C. Ochsenfeld, S.T. Brown, et al., Advances in methods and algorithms in modern quantum chemistry program package, Phys. Chem. Chem. Phys. 8 (27) (2006) 3172–3191.
[35] C.W. Yap, PaDEL-descriptor: an open source software to calculate molecular descriptors and fingerprints, J. Comput. Chem. 32 (7) (2011) 1466–1474.
[36] B. Ruscic, Active thermochemical tables: sequential bond dissociation enthalpies of methane, ethane, and methanol and the related thermochemistry, J. Phys. Chem. 119 (28) (2015) 7810–7837.
[37] F. Sun, R. Jin, Theoretical study on the radical scavenging activity of shikonin and its ester derivatives, Res. J. Appl. Sci. Eng. Technol. 6 (2) (2013) 281–284.
[38] D. Mikulski, K. Eder, M. Molski, Quantum-chemical study on relationship between structure and antioxidant properties of hepatoprotective compounds occurring in cynarascolymus and silybum marianum, J. Theor. Comput. Chem. 13 (1) (2014) 1–24.
[39] M. Najafi, K.H. Mood, M. Zahedi, E. Klein, DFT/B3LYP study of the substituent effect on the reaction enthalpies of the individual steps of single electron transfer–proton transfer and sequential proton loss electron transfer mechanisms of chroman derivatives antioxidant action, Comput. Theor. Chem. 969 (2011) 1–12.
[40] N. Nenadis, M.Z. Tsimidou, Contribution of DFT computed molecular descriptors in the study of radical scavenging activity trend of natural hydroxybenzaldehydes and corresponding acids, Food Res. Int. 48 (2012) 538–543.
[41] J.E. Bartmess, Thermodynamics of the electron and the proton, J. Phys. Chem. 98 (1994) 6420–6424.
[42] M.M. Bizarro, B.J.C. Cabral, R.M.B. Santos, J.A.M. Simoes, Substituent effects on the O–H bond dissociation enthalpies in phenolic compounds: agreements and controversies, Pure Appl. Chem. 71 (7) (1999) 1249–1256.
[43] J. Rimarcik, V. Lukes, E. Klein, M. Ilcin, Study of the solvent effect on the enthalpies of homolytic and heterolytic N–H bond cleavage in p-phenylenediamine and tetracyano-p-phenylenediamine, J. Mol. Struct. 952 (2010) 25–30.
[44] Y. Li, M. Toscano, G. Mazzone, N. Russo, Antioxidant properties and free radical scavenging mechanisms of cyclocurcumin, New J. Chem. 42 (15) (2018) 12698–12705.
[45] A. Bayat, A. Fattahi, The free radical scavenging activity of lespedezacoumestan toward OH radical: a quantum chemical and computational kinetics study, J. Phys. Org. Chem. 31 (2) (2017), e3755.
[46] A. Amic, B. Lučić, V. Stepanić, Z. Marković, S. Marković, J. DimitrićMarković, D. Amić, Free radical scavenging potency of quercetin catecholic colonic metabolites: thermodynamics of 2H+/2e- processes, Food Chem. 218 (2017) 144–151.

[47] Y.Z. Zheng, G. Deng, Q. Liang, D.F. Chen, R. Guo, R.C. Lai, Antioxidant activity of quercetin and its glucosides from propolis: a theoretical study, Sci. Rep. 7 (2017) 7543.
[48] M.D. Tissandier, K.A. Cowen, W.Y. Feng, E. Gundlach, M.H. Cohen, A.D. Earhart, J.V. Coe, T.R. Tuttle Jr., The proton's absolute aqueous enthalpy and Gibbs free energy of solvation from cluster-ion solvation data, J. Phys. Chem. 1*02* (40) (1998) 7787–7794.
[49] S. Hwang, D.S. Chung, Calculation of the solvation free energy of the proton in methanol, Bull. Kor. Chem. Soc. 26 (2005) 589–593.
[50] J.J. Fifen, Z. Dhaouadi, M. Nsangou, O. Holtomo, N. Jaidane, Proton-coupled electron transfer in the reaction of 3,4-dihydroxyphenylpyruvic acid with reactive species in various media, Int. J. Chem. Phys. 2015 (2015) 1–13.
[51] Y. Xue, Y. Zheng, L. An, Y. Dou, Y. Liu, Density functional theory study of the structure–antioxidant activity of polyphenolic deoxybenzoins, Food Chem. 151 (2014) 198–206.
[52] G. Wang, Y. Xue, L. An, Y. Zheng, Y. Dou, L. Zhang, Y. Liu, Theoretical study on the structural and antioxidant properties of some recently synthesised 2,4,5-trimethoxy chalcones, Food Chem. 171 (2015) 89–97.
[53] D.O. Işın, Theoretical study on the investigation of antioxidant properties of some hydroxyanthraquinones, Mol. Phys. 114 (24) (2016) 3578–3588.